BOREAL ENVIRONMENT RESEARCH 25: 105–120
ISSN 1797-2469 (online)

Helsinki 14 October 2020

Extensive accumulation of rare earth elements in estuarine sediments affected by leaching of acid sulfate soils

Mats E. Åström1)*, Changxun Yu1), Joonas J. Virtasalo2), Peter Österholm3), Pasi Peltola1), Edward D. Burton4), K. Johan Hogmalm5) and Antti E. K. Ojala2)

1) *Department of Biology and Environmental Science, Linnaeus University, SE-39182 Kalmar, Sweden (*corresponding author's e-mail: mats.astrom@lnu.se)*
2) *Geological Survey of Finland (GTK), PO Box 96, FI-02151 Espoo, Finland*
3) *Abo Akademi University, Department of Geology, FI-20500 Åbo, Finland*
4) *Southern Cross GeoScience, Southern Cross University, PO Box 157, Lismore, NSW 2480, Australia*
5) *Department of Earth Sciences, University of Gothenburg, SE-405 30 Gothenburg, Sweden*

Received 6 Apr. 2020, final version received 16 Sep. 2020, accepted 14 Sep. 2020

Åström M.E., Changxun Y., Virtasalo J.J., Österholm P., Peltola P., Burton E.D., Hogmalm K.J. & Ojala A.E.K. 2020: Extensive accumulation of rare earth elements in estuarine sediments affected by leaching of acid sulfate soils. *Boreal Env. Res.* 25: 105–120.

The concentrations, loads and speciation of rare earth elements (REEs) were studied in a 3.5 m thick mud depositional succession from an estuary in the Gulf of Bothnia. The uppermost 182.5 cm of the mud, estimated to have deposited from the early 1970s to 2011 (sampling year), had very high REE concentrations (596−1456 ppm) and accumulation rates (5.2−28 g m^{-2} year^{-1}). This was explained by large REE export from acid sulfate soils after they became efficiently drained with modern drainage techniques. Geochemical and synchrotron-based spectroscopic (XANES) analyses showed that the REEs in the mud are relatively firmly bound in non-clastic phases, likely adsorbed by clay minerals and also to some extent by iron oxyhydroxides. Below 182.5 cm, the REE concentrations successively decreased down to background values at the base at 3.5 m, reflecting less efficient drainage and leaching of the acid sulfate soils in previous decades and centuries.

Introduction

The concentrations of dissolved rare earth elements (REE) are typically inversely correlated with pH in natural waters (Sholkovitz 1995, Lawrence *et al.* 2006). Hence, the ∑REE concentrations (all 14 REEs including La-Lu) in low-pH waters are consistently elevated (Noack *et al.* 2014, Wallrich *et al.* 2020) and in strongly acidified waters, they can reach up to several mg/L (Gammons *et al.* 2003, da Silva *et al.* 2009, Lecomte *et al.* 2017, Olias *et al.* 2018) and in extreme cases, upwards to 100 mg/L (Moraes *et al.* 2020). The typically large, dissolved REE pool in acidic waters will consistently diminish (be removed) downstream where pH increases as a result of proton-buffering reactions or extensive dilution (Sholkovitz 1995, Borrego *et al.* 2012). This pH-related REE-removal process may, as shown in field and experimental studies with strong pH gradients, involve REE partitioning into a variety of phases: including Fe oxyhydroxides (Protano and Riccobono 2002, Verplanck *et al.* 2004, Gammons *et al.* 2005a, Delgado *et al.*

Editor in charge of this article: Anu Kaakinen

2012, Morgan *et al.* 2016, Lecomte *et al.* 2017), organic matter (Astrom *et al.* 2012, Morgan *et al.* 2012), Al hydroxides (Gammons *et al.* 2005b, Wood *et al.* 2006, Astrom *et al.* 2012, Delgado *et al.* 2012, Li and Wu 2017, Stewart *et al.* 2017), aluminium-sulfates/basaluminite (Ayora *et al.* 2016, Soyol-Erdene *et al.* 2018, Lozano *et al.* 2019, Lozano *et al.* 2020) and Al_{13}-polymers (Moraes *et al.* 2020). Yet other phases with known potential to bind or incorporate REEs may also be potentially involved, such as phyllosilicates (Tertre *et al.* 2008, Gladysz-Plaska *et al.* 2014), calcite (Zhong and Mucci 1995) and phosphates (Edahbi *et al.* 2018). A large variety of REE-removal mechanisms is therefore possible, but in most natural pH-neutralisation systems, difficult to distinguish from one another as increasing pH typically involve formation and preservation of several of the potential REE-scavenging phases.

An acidic setting in which REEs are exceptionally mobile, but which in terms of REE geochemistry has received much less attention than acid-mine drainage environments, is soils that are widespread on coastal plains and referred to as acid sulfate soils. These soils develop when the groundwater table drops as a result of artificial drainage (e.g. ditching for farming purposes) or natural drainage (e.g. postglacial isostatic land uplift) of fine-grained calcite-poor sediments (mostly Holocene) containing pyrite and/or metastable Fe sulfides (Dent and Pons 1995, Mosley *et al.* 2014). Whereas the total REE concentrations of the acid sulfate soils are not typically substantially elevated as compared with other soils/sediments (Astrom *et al.* 2010, Sukitprapanon *et al.* 2019), the pore water of these soils can have very high ∑REE concentrations of up to 10 mg/L (Welch *et al.* 2009, Astrom *et al.* 2010, Groger *et al.* 2011). Consequently, ∑REE concentrations are typically very high also in recipients and materials affected by these soils, such as creeks (Astrom 2001, Jones *et al.* 2016), suspended particulate matter (Astrom *et al.* 2012) and benthic sediments (Nordmyr *et al.* 2008b, Morgan *et al.* 2012, Morgan *et al.* 2016). Taken together, these studies suggest that REEs are released in large amounts in the acid sulfate soils, transported downstream in dissolved form by the acidic waters, and ultimately are removed from the dissolved phase as pH increases in recipients. These mechanisms are in line with REE behaviour in other environments where the main driving force of acidification is mining activities (Gammons *et al.* 2003, Verplanck *et al.* 2004, Lecomte *et al.* 2017) or natural volcanic processes (Gammons *et al.* 2005b). There is, however, limited information regarding REE abundance and speciation in estuarine sediments affected by neutralisation of acidic REE-rich waters, in particular where such waters are derived from acid sulfate soils. As a consequence, the ultimate solid-state forms and behaviour of REEs in such sedimentary settings are poorly known, and therefore sedimentary REE profiles have seldom been utilised to trace and quantify historical and current metal loadings from acidified metal-delivering terrestrial environments, such as acid sulfate soil landscapes.

The main aim of this study was to determine the vertical variability in the concentrations, loads and speciation of REEs in the estuarine sediment of a creek that is periodically acidified and enriched in REEs as a result of leaching of acid sulfate soils. The study builds on a 3.5 m thick estuarine mud depositional succession that was characterised in terms of REE concentrations via high-resolution sampling, and REE speciation by combining a 7-step sequential chemical extraction (SCE) with synchrotron-based X-ray absorption near-edge structure (XANES) spectroscopy. The study is an extension of our previous studies in this setting focusing on REEs in soils and waters within the creek's catchment (Astrom *et al.* 2010) and REEs in suspended particulate matter in the creek's estuary (Astrom *et al.* 2012).

Methods

Field Site

The field site was the low-salinity (< 6‰) estuary of the Vörå creek located in the eastern parts of the Gulf of Bothnia in the northern part of the Baltic Sea (Fig. 1). This perennial creek has a catchment area of 223 km^2 with a mean annual flow of 7–9 l s^{-1} km^{-2} (Nordmyr *et al.* 2008b). It runs through a landscape rich in

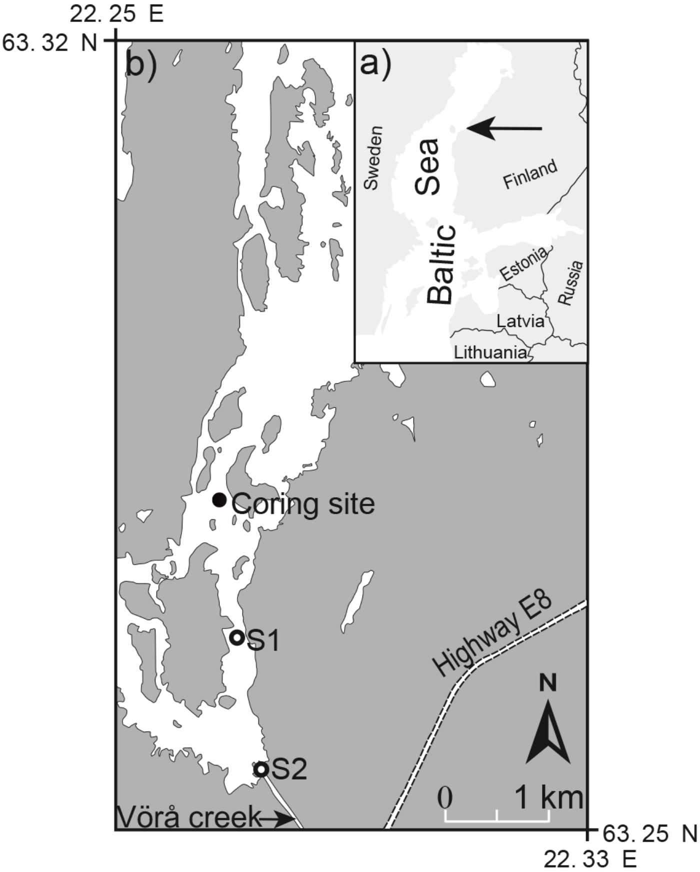

Fig. 1. Map location of the (**a**) field site and (**b**) of the estuary showing the location where the four parallel sediment cores (Coring site) were taken and the water samples for extraction of suspended particulate matter (S1 and S2, respectively) were collected. The figure is reproduced from Yu *et al.* (2015).

acid sulfate soils (approximately 20%), which are typically 1–2 m thick and formed in Holocene sulfide-bearing marine (brackish-water) sediments (Yli-Halla *et al.* 1999, Boman *et al.* 2010). As a consequence of leaching of these soils, the Vörå creek is frequently very acidic (median pH: 4.5) and has high concentrations of ∑REEs (median: 175 µg L^{-1}) (Astrom *et al.* 2010) and other metals (Nordmyr *et al.* 2008b), leading to high ecotoxicological risks (Wallin *et al.* 2015). Other parts of the catchment are covered mainly by histosols (peat), and podzols developed on till deposited during the melting of the Weichselian glaciation in the late Pleistocene. The estuary is shallow (< 20 m deep), non-tidal and well-sheltered from wave action by surrounding land areas and islands. In this estuary, the REEs transported by the acidic creek are removed from the dissolved phase as pH increases, resulting in high REE concentrations in suspended particulate matter of up to 1700 ppm (Astrom *et al.* 2012). From December to April, the catchment and estuary are covered by ice and snow. The annual mean temperature in the area is 3°C and the mean annual precipitation is approximately 500 mm.

Sampling

Based on a general understanding of water currents and on knowledge from previous studies in the estuary (Nordmyr *et al.* 2008a, Nordmyr *et al.* 2008b, Astrom *et al.* 2012), a sediment-coring site with a water depth of approximately 15 m was selected in the central part of the estuary (Fig. 1). The sampling was carried out with a Kullenberg-type piston corer mounted on the ice in late winter (March) 2011. In order

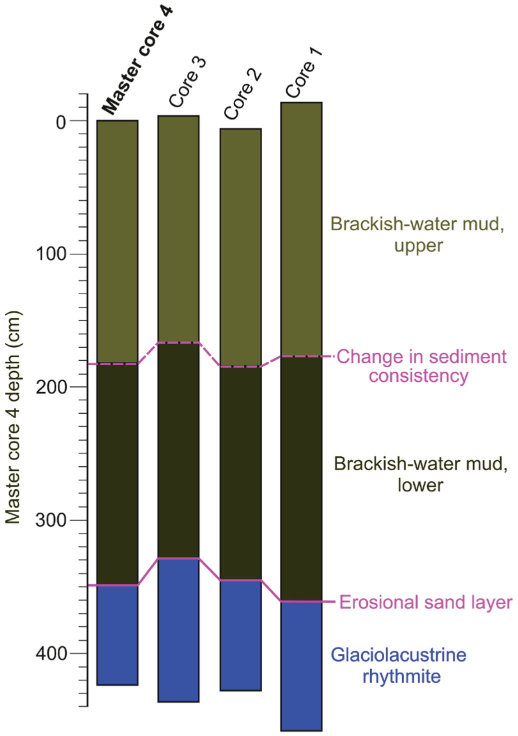

Fig. 2. Simplified stratigraphic features and core-core correlation, with the studied mud depositional succession indicated. The basal (glaciolacustrine) rhythmites below the erosional sand layer accumulated before 9000 years ago and are not further considered. Change in sediment consistency denotes significantly increased softness and water content of the sediment above this depth. The figure is reproduced from Yu *et al.* (2015).

to get enough material for the entire analytical scheme, four parallel cores (denoted as Core1, Core2, Core3, Master core4) with lengths between 4 m and 5 m were collected within an area of approximately 40 cm x 100 cm. To transport the samples to the laboratory, the cores were cut and sealed in approximately 2.5 m long sections. The core-to-core correlation, sedimentological and geophysical/mineralogical features, major-element chemistry and age-depth relationships are reported in previous papers (Yu *et al.* 2015, Yu *et al.* 2016b, Yu *et al.* 2016a). Simplified stratigraphic features, core-core correlation, and the length of the studied mud depositional succession are presented in Fig. 2.

During high-water flow in autumn (December), surface water was collected from the inner estuary (S1; pH 5.0) and the mouth (S2; pH 4.4) of the creek (Fig. 1) using acid-washed polypropylene bottles. Thereafter, the suspended particulate matter in these waters was obtained by centrifugation and air-dried.

Chemical analyses of field samples

Segments with a thickness of 2 cm (10 cm below 3.5 m) collected from one of the replicate cores were dried and sent to Acme Analytical Laboratories Ltd. (ISO 9001 accredited) for analysis of total REE concentrations. A 20 mL aliquot of an acid solution (2:2:1:1 H_2O-HF-$HClO_4$-HNO_3) was added to a pulverised sample split of 0.25 g, which was heated until fuming on a hot plate and taken to dryness. A 16 mL aliquot of 50% HCl was then added to the residue and heated in a hot-water bath (~95°C) for 30 min. After cooling, the solution was transferred to a 100 mL volumetric flask and made to volume using 5% HCl and analysed by Inductively Coupled Plasma Mass Spectrometry (ICP-MS). Analyses of blanks were carried out to measure background, duplicates to monitor analytical precision, and reference materials (internal laboratory reference materials) to determine accuracy and concentrations. Additionally, the samples were analysed in random order (i.e. not according to sampling depth), and blind duplicates showed that the analytical error was much smaller than the natural concentration variability in the sample material. Hence, the identified depth-related concentration-variation patterns are real features.

Twelve 8-cm-thick segments sampled at selected depth intervals from one of the replicate cores were subjected to a 7-step SCE. To prevent any oxidation during transportation, these segments were stored in anaerobic jars with Anaerocult A (http://www.merckmillipore.com/), which can chemically bind oxygen quickly and completely, producing a CO_2-rich oxygen-free (anaerobic) atmosphere. The extractions were performed on wet subsamples corresponding to approximately 1 g of dry material with 40 ml deoxygenated solutions (produced by purging solutions with highpurity N_2 for at least 1 h) in an anaerobic chamber (95% N_2 + 5% H_2) maintained at < 1 ppm O_2 with a Pd catalyst. Agitation and centrifugation were conducted outside the anaerobic chamber in air-tight vials. All extraction steps were conducted at room temperature except SCE-7, which was performed on a hot plate at approximately 95°C. The SCE was performed on 3 replicate subsamples. The steps are as follows:

1. 1 M NH_4NO_3 for 2 h; water soluble and easily exchangeable (Scheinost *et al.* 2002)
2. 1 M CH_3COONH_4 at pH 6 for 4 h; carbonates and weak organic complexes (Scheinost *et al.* 2002)
3. 0.1 M NH_2OH-HCl combined with 1 M CH_3COONH_4 at pH 6 for 0.5 h; Mn oxides and weak dissolution of Fe oxyhydroxides if present in large amounts (Neaman *et al.* 2004)
4. 1 M HCl for 4 h; Al oxyhydroxide, metastable Fe sulfides and Fe oxyhydroxides (Claff *et al.* 2010) and some sheet silicates (Haese *et al.* 1997)
5. 0.35 M CH_3COOH/0.2 M $C_6H_5Na_3O_7$ buffer with 50 g L^{-1} $Na_2S_2O_2$ for 4 h; crystalline Fe-oxides
6. Concentrated HNO_3 for 2 h; pyrite (Claff *et al.* 2010)
7. EPA method 3050 consisting of hot acid and peroxide; recalcitrant minerals

After each extraction, the solutions were centrifuged and the supernatants were filtered through 0.45-µm filters and acidified to pH < 2 with ultrapure HNO_3. The concentrations of REEs in the supernatants were determined on an Agilent 7500 ICP-MS. Solutions were diluted 25 times in 5% HNO_3, and an internal standard solution containing 800 ppb indium and rhenium was added to the samples prior to measurement. Serial dilutions of multi element standard solutions (Merck and Agilent) were analysed to construct linear calibration graphs. Drift and accuracy were monitored by analysis of dissolved rock standards JB-1 and W-1. The analytical precision for the REEs was generally better than 5%, while accuracy was within 5−10%. The data are presented as the mean ± standard deviation of the triplicate determinations.

XANES analyses of field samples

Synchrotron-based XANES spectroscopy carried out at MAX-lab, Lund University, Sweden, was used to qualitatively assess the solid-phase speciation of Ce in six samples of the mud and the two samples of suspended particulate matter. The X-ray beam was scanned over the Ce L_{III} absorption edge and the retrieved XANES spectra of the samples were compared with corresponding spectra collected for references. The latter included CeO_2, $Ce(OH)_4$, aqueous Ce^{3+}, $Ce_2(CO_3)_3$, and Ce(III) sorbed by clay, humic acid, Al hydroxide and 2-line ferrihydrite. The XANES analyses were carried out according to standard procedures (Lombi and Susini 2009, Manceau and Matynia 2010, Edahbi *et al.* 2018) and are summarized in the Supplement.

Experiment on REE sorption on clays

A 3-step SCE consisting of three selected steps of the 7-step SCE scheme (nos. 2, 4 and 6) was applied on La- and Pr-loaded illite, ripidolite and illite-smectite mixed layer clay (purchased from the Clay Minerals Society, Purdue University). These three steps are referred to as Exp_step-1, Exp_step-2 and Exp_step-3, respectively. Briefly, 500 mg triplicate samples of finely pulverised mineral (illite, ripidolite and illite-smectite mixed-layer clay) were mixed with 0.0005 M La and Pr stocking solutions. The pH of the suspensions was adjusted to 6.5. Modelling with VISUAL MINTEQ predicted that the dissolved La and Pr occurred as free cations under the experimental conditions. After shaking overnight, the suspensions were centrifuged and the obtained solid materials were washed five times with MQ water (in order to remove excess La and Pr) and then sequentially extracted. La and Pr, and Ce (as a proxy for REEs naturally bound to the clays), were measured in the extractants using the same analytical set-up as in the 7-step SCE scheme. The results are presented as mean concentrations ± the standard deviation.

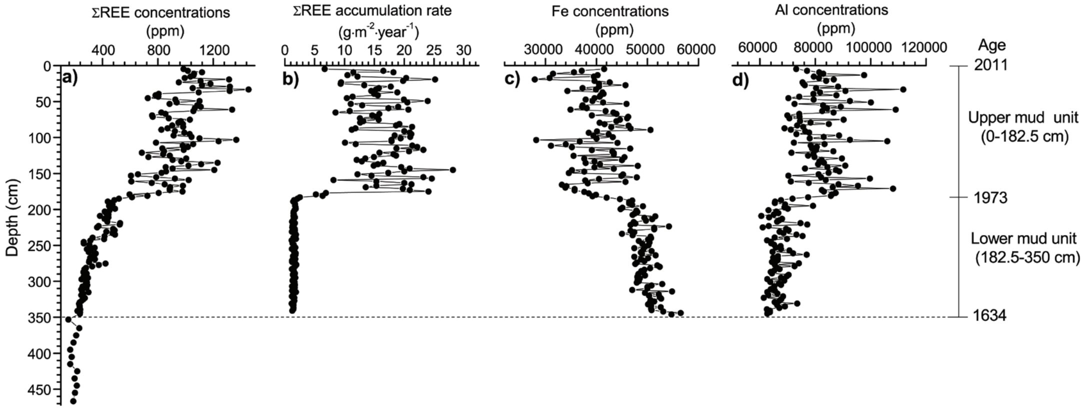

Fig. 3. The (**a**) total ∑REE concentrations, (**b**) accumulation rates and total concentrations of (**c**) Fe and (**d**) Al in the mud depositional succession. The Fe and Al data are from an earlier work (Yu *et al.* 2015, Yu *et al.* 2016b). The age-depth model is based on ^{137}Cs accumulation for the upper unit and radiocarbon dating for the lower unit, as discussed in detail in Yu *et al.* (2015). The sedimentation rate is on average approximately 5 cm year^{-1} for the upper mud unit and, although less constrained, approximately 0.5 cm year^{-1} for the lower mud unit (Yu *et al.* 2015).

Results and Discussion

General features of the mud depositional succession

The mud depositional succession was 3.5 m thick in the Master core4 (Fig. 2). It was characterised by an abrupt change in consistency at 182.5 cm (Fig. 2), which does not represent a break in sedimentation as indicated by visual inspection of the sediment core and analysis of X-radiographs (Yu *et al.* 2015). The unit above 182.5 cm, referred to as the "upper mud unit", was based on ^{137}Cs accumulation estimated to have deposited between 1973 and 2011 (core top) at an average sedimentation rate of 5 cm year^{-1} (Yu *et al.* 2015). The unit below this depth, referred to as the "lower mud unit" and divided from the upper mud unit by the Boundary function (OxCal v4.2, Ramsey 2009) (Yu *et al.* 2015), has a less well-constrained age but is, based on radiocarbon dating, interpreted to have been deposited from 1973 to approximately four centuries ago at an average sedimentation rate of 0.5 cm year^{-1} (Yu *et al.* 2015). Below 3.5 m, there were basal (glaciolacustrine) rhythmites (Fig. 2) that accumulated before 9000 years ago (Stroeven *et al.* 2016). These are not further considered here.

REE abundance in the mud — the effect of acid sulfate soils

At the base of the mud depositional succession, ∑REE concentrations were 220–240 ppm (Fig. 3a) and La concentrations were 45–50 ppm (Table S1 in the Supplement). Similar sediments occur in low-lying near-coastal terrestrial landscapes in the region due to extensive land uplift in the Holocene, related to the melting of the thick Weichselian continental glaciation in the late Pleistocene. In these sediments, sampled at several hundred sites in a mapping project, the 10th and 90th percentiles of the La concentrations were 25 ppm and 50 ppm, respectively (Astrom and Bjorklund 1997). Hence, the base of the mud had REE concentrations corresponding to background levels for this kind of sediment in this region. A main part of the REEs deposited in the mud in these times (17th century) was certainly bound in mobilized/leached fine fractions of till, which is the dominating regolith type in the region and formed by redistribution of older (Pleistocene) unconsolidated deposits and erosion of the crystalline bedrock (dominated by Proterozoic granitoids and gneisses) during the Weichselian glaciation.

During the relatively slow formation of the lower mud unit (from approximately four centuries ago to the early 1970s), the REE concentrations successively increased (Fig. 3a). During this period, there was an increase in artificial drainage of wetlands, carried out in order to increase the area of agricultural land for a growing population. As the wetlands were frequently underlain with fine-grained calcite-poor sediments (mostly Holocene) containing pyrite and/or metastable Fe sulfides (Boman *et al.* 2010), acid sulfate soil development and associated increase in acidity formation and metal release were inevitable (Astrom *et al.* 2005). This certainly resulted in increased acidification and metal (e.g. REE) loading of a number of watercourses (Roos and Astrom 2005), including the Vörå creek studied here. Consequently, as the water of the Vörå creek flowed into the estuary, its pH increased leading to REE removal from the dissolved phase (Astrom *et al.* 2012) and thus ultimately to REE accumulation in the mud. Hence, the successive increase in REE concentrations upwards in the lower mud unit is evidence of increased development and leaching of acid sulfate soils.

In the upper mud unit, the ∑REEs occurred in highly elevated concentrations (596–1456 ppm) in a zigzag-like manner (Fig. 3a) and had accumulated at exceptionally high rates (5.2–28 g m^{-2} $year^{-1}$) (Fig. 3b) (data given in Tables S1 and S2 in the Supplement). This is certainly a result of extensive leaching of acid sulfate soils — occurring mainly under farmlands reclaimed by drainage of wetlands, as there are no other natural or anthropogenic REE sources in the region. Additionally, similar ∑REEs concentrations occur in sediments affected by acid sulfate soils in subtropical Australia (Xu *et al.* 2018). The reason as to why the acid sulfate soils started to deliver increasingly stronger amounts of REEs as well as other metals, like Al (Yu *et al.* 2016b) and Be (Astrom *et al.* 2018) from the early 1970s onwards is that the farmlands were drained both by deeper/cleaner open ditches and by newly constructed subsurface-drainage systems consisting of decimeter-wide plastic pipes at depths of approximately one meter. The combined effect of these two modern drainage activities is that, first, the groundwater table drops further, causing an increase in metal-sulfide oxidation and thus soil acidification and associated metal release. Second, the rain and snow-melt water is efficiently discharged from the fields, which increases the rate and export of acidity and metals. The ultimate result is, as recorded here, strongly elevated REE concentrations and accumulation rates in the recipient (estuarine) mud.

In summary, the formation of acid sulfate soils within the Vörå creek catchment has had a long-lasting and increasing impact on the REE abundance in the mud deposited in the creek's estuary. Consequently, while the agricultural activities turned the wetlands into productive farmlands benefiting the local community, they also deteriorated the surface-water quality (Sundstrom *et al.* 2002) and resulted in contamination of the estuarine sediments with REEs (Fig. 3) and other metals. In order to gain a mechanistic understanding of the REE accumulation and preservation in the mud; and environmental information regarding how potentially mobile the sedimentary REE pool is, the solid-phase REE speciation was determined, primarily on samples from the upper mud unit that faces the sediment-water interface, which is the most contaminated unit.

REE solid-phase speciation in the contaminated upper mud unit

In the upper-mud unit, the REEs were released largely in the 4th SCE step, consisting of 1 M HCl (84–86%), and thus to only a small extent in the other six steps (Fig. 4). High 1 M HCl extractability has also been found previously for REEs in sediments affected by acid sulfate soil in the subtropical zone (Morgan *et al.* 2012, Morgan *et al.* 2016). When normalised to the North American Shale Composite (NASC) composition (Haskin 1968, Gromet *et al.* 1984), the REEs extracted by 1 M HCl (step 4) displayed a flat trend from La to Sm, a negative Eu anomaly and a slope from Gd to Lu (Fig. 5). A similar fractionation pattern was recorded for the REEs extracted at steps 2 and 3 (Fig. 5). Profoundly different patterns occurred for the REEs released by the other steps, including step 1 with an overall flat pattern, step 5 with a medium-weight REE enrichment, and steps 6 and 7 with a slope throughout the REE series (Fig. 5). Taken together, these data show that: 1) the REEs

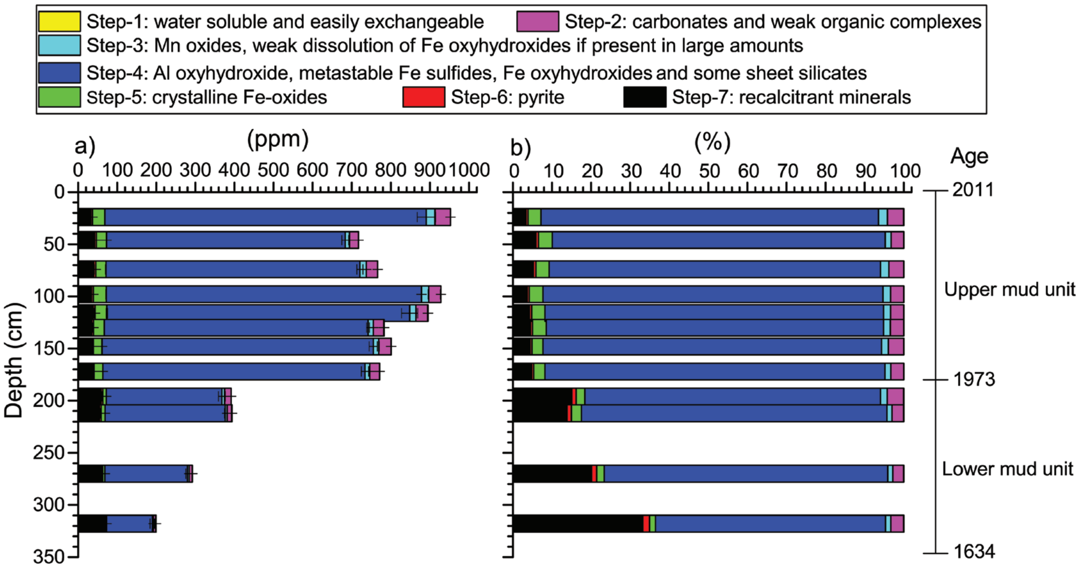

Fig. 4. The (**a**) concentrations (ppm) and (**b**) proportions (%) of ∑REEs extracted at each step of a 7-step sequential chemical extraction applied on 12 segments from the mud depositional succession. The chemical regents and analytical procedures are given in the main text.

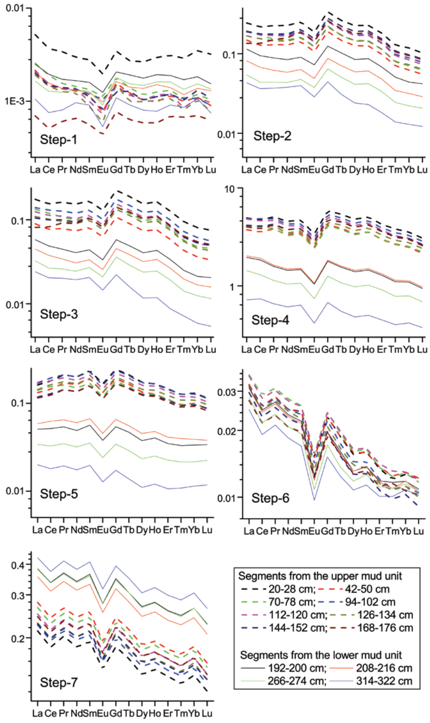

Fig. 5. REEs extracted in each step of a 7-step sequential chemical extraction on 12 segments from the mud normalised against the North American Shale Composite (NASC) composition (Haskin 1968, Gromet *et al.* 1984). The chemical reagent and targeted minerals and phases for each step are given in the main text.

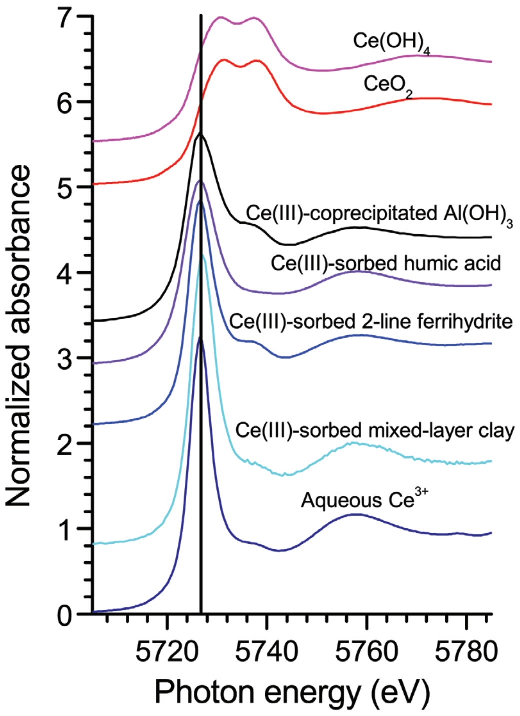

Fig. 6. Cerium L_{III}-edge XANES spectra of relevant reference compounds with the position of white lines for trivalent Ce (black vertical line) indicated.

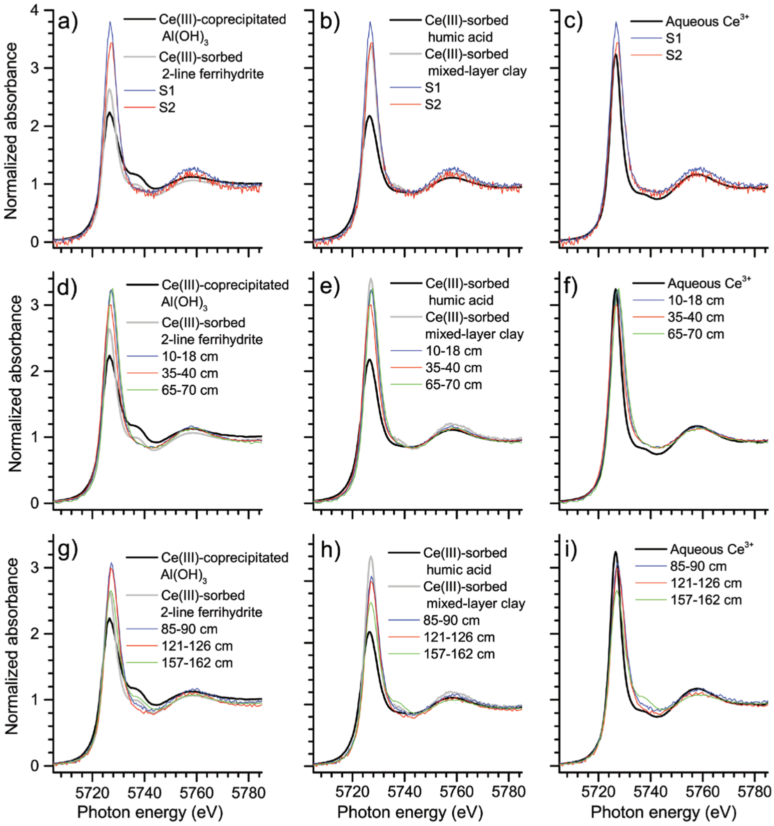

Fig. 7. Cerium L$_{III}$-edge XANES spectra of relevant reference compounds and of the suspended particulate matter (S1 and S2, respectively) and six sediment segments from various depths.

were to a large extent bound in non-clastic (1 M HCl-extractable) phases; 2) the REEs were, to only a minor extent, occurring in phases that are extracted with the relatively weak (and pH circumneutral) reagents applied in the first three SCE steps; and 3) the distinct fractionation patterns showed that the applied chemical reagents were in general able to discriminate between various REE phases, perhaps with the exception of steps 2 and 3 that may have extracted a portion of the dominating REE phase(s) abundantly released at step 4.

In an attempt to acquire more information on the nature of the REE specie(s) abundantly extracted with the 4th SCE step (1 M HCl), Ce L$_{III}$-edge XANES spectroscopy was carried out on six samples of the upper mud unit and on the two samples of suspended particulate matter from the estuarine/creek water. The XANES spectra showed that in all eight samples, Ce existed overwhelmingly, or entirely, in the trivalent oxidation state, because all samples had a major single peak (white line) at the same photon energy as the Ce(III) reference compounds (5727 eV) but no signs of a double peak at higher photon energies characteristic for the Ce(IV) references (Figs. 6 and 7). Therefore, the data for Ce is representative for the other 13 REEs that have only a +III state (except for Eu that may also occur as +II). Considering the relatively large variability in XANES spectral features among the references (Fig. 6), the overall similarity in spectral features among all the eight samples, except for some variability in the magnitude of the white-line peak (Fig. 7a, d, and g), indicated a relatively homogeneous REE speciation in the upper mud unit and the suspended particulate matter. The nature of this REE speciation is evaluated next.

Organic matter, which can form strong complexes with REEs (Pourret *et al.* 2007, Pourret and Martinez 2009, Tang and Johannesson 2010, Marsac *et al.* 2011), occurred in higher concentrations in the upper than the lower mud unit (Yu *et al.* 2015) in a manner similar to the REEs (Fig. 3a). These two variables were thus correlated in the mud depositional succession. Whereas the organic matter and REEs have different sources, that is, the latter are derived mainly from the acid sulfate soils located under farmland and the former mainly from peat and humus horizons in forested areas (Astrom *et al.* 2010), they can hypothetically become attached when waters from these two kinds of soil materials mix within the creek or in the estuary. The XANES spectra of the Ce(III)-sorbed humic acid reference was, however, distinctly different (i.e. a much weaker white-line peak) from all the samples of the mud and suspended particulate matter, indicating that humic substances are not a major scavenger of the REEs in this sediment. This is consistent with previous findings that: 1) organic matter in estuarine sediments across Europe and elsewhere has overall relatively low concentrations of ∑REEs (median: 74 ppm) with a pronounced depletion of the light (La-Nd) and heavy (Dy-Lu) REEs as compared to the medium-weight (Sm-Tb) REEs (Freslon *et al.* 2014); a fractionation feature not found for the REEs in the mud studied here (Fig. 5); and 2) REEs bound to precipitates formed via experimental mixing of extremely acidic (pH 1.7) and REE-rich (> 11 mg/L) Tinto River water and sea water are not, according to results of sequential chemical extractions, attached to organic matter (Lecomte *et al.* 2017).

Aluminium had concentration-variation patterns (enrichment in the upper mud unit) and extractability features (largely extacted by 1 M HCl) similar to those of the REEs in the mud depositional succession (Fig. 3, Tables S1 and S3 in the Supplement). Aluminium is also, like the REEs, abundantly leached from acid sulfate soils and precipitate in the estuary when the acidic creek water is neutralised via mixing with sea water (Astrom *et al.* 2012). A relationship between Al and REEs has been found also elsewhere where acidic river water is neutralised (Gammons *et al.* 2005b, Wood *et al.* 2006, Ogawa *et al.* 2019), and is principally a result of a common response to pH, that is, both Al and the REEs are highly soluble in acidic waters (like here in the creek) but are transformed to particulate phase under near-neutral conditions (like here in the estuary). As a consequence, binding of REEs by freshly precipitated Al hydroxides may easily occur, and is supported by evidence of capacity of Al hydroxides to bind REEs (Quinn *et al.* 2004, Brito *et al.* 2018). The XANES spectra of the Ce(III)-coprecipitated $Al(OH)_3$ reference had, however, distinctly different features to both the mud and suspended particulate matter, including a significantly weaker white-line peak and a much stronger shoulder at 5735 to 5741 eV (Fig. 7). These spectral features thus suggest that Al hydroxides are not a major scavenger phase of the REEs, which is in line with previous studies showing that Al-flocs account for only approximately 10% of the REE removal during neutralisation in a Cu-Pb-Zn mining area (Protano and Riccobono 2002).

Iron displayed concentration variations that were almost opposite to those of the REEs, such that it occurred in lower concentrations in the upper than the lower mud unit (Fig. 3, Table S1 in the Supplement). Furthermore, Fe was extracted to only approximately 40% by 1 M HCl in the upper mud unit, which was not higher than in the lower unit (Yu *et al.* 2015) (Table S3 in the Supplement). These sedimentary features of Fe are largely explained by extensive retention, and thus relatively limited leaching, of the Fe released from minerals (metal-sulfides and phyllosilicates) in the acid sulfate soils (Osterholm and Astrom 2002, Sohlenius and Oborn 2004). These geochemical differences between Fe and REEs are, however, not conclusive evidence that Fe phases are not major carriers of the REEs in the mud and suspended particulate matter. The reason is that Fe is a major constituent in these materials and a significant fraction of the total Fe in the mud (10-24%) occurs as 2-line ferrihydrite (Yu *et al.* 2015) with high sorptive capacity. A Ce(III)-sorbed 2-line ferrihydrite reference was accordingly made, but had in contrast to the samples, a considerably weaker white-line peak and a shoulder at 5735 eV to 5741 eV (Fig. 7). The exception was one mud sample at a depth of 157−162 cm that had a spectrum very similar to that of the ferrihydrite reference (Fig. 7g). These features indicate that sorption of REEs to Fe oxyhydroxides (ferrihydrite) may not be important in the upper-mud unit in general, like in passive-remediation treatment of acid mine drainage where schwertmannite does not accumulate REEs (Ayora *et al.* 2016), but can be important at certain depths. The latter feature is in line with the high capacity of Fe oxyhydroxides to scavenge REEs as documented both in laboratory experiments (Bau 1999, Quinn *et al.* 2006) and under many kinds of field conditions (Sholkovitz *et al.* 1992, Protano and Riccobono 2002, Verplanck *et al.* 2004, Johnston *et al.* 2015), and also with identification of a porous Fe-La phase (La/Fe/O = 1:1:3) in corresponding acid sulfate soil affected sediments in subtropical Australia (Xu *et al.* 2019). Metastable Fe sulfides, in which Fe exists as +II, are also relatively abundant in the mud (0.26–0.73% of dry sediment weight) (Yu *et al.* 2015) and have been suggested as potential REE carriers in marine sediments (Chaillou *et al.* 2006). Despite this, there are no reasons to suggest that metastable Fe sulfides, which were not included as a reference in the XANES analyses, are significant REE carriers because: 1) for the suspended particulate matter, in which sulfides cannot exist due to oxidising conditions, the XANES spectra were similar to those of the mud (Fig. 7); 2) sulfides are secondary phases in the mud and can therefore not have been involved in the REE removal process in the estuarine waters; 3) REEs are lithophile metals typically not associated with sulfur; and 4) an experiment carried out with corresponding sediments from subtropical Australia showed that REEs exhibit little (or no) short-term sorptive affinity for Fe sulfide (Morgan *et al.* 2012).

Cerium(III)-sorbed mixed-layer clay was the reference with a XANES spectra most similar to those of the suspended particulate matter and all the mud samples except the deepest sample at 157–162 cm (Fig. 7b, e, and h). This was supported by linear combination fitting (LCF), a frequently applied approach by which the sample spectrum is fitted with a linear combination of the reference spectra in order to quantify the species composing a sample (Lombi and Susini 2009, Grafe *et al.* 2014). The result of the LCF revealed that Ce(III)-sorbed mixed-layer clay accounted for 100% binding of the REEs in the suspended particulate matter and 67–93% binding for five out of six mud samples (last mud sample: 44%). Although the LCF results should be seen as indicative as they can contain relatively large errors due to many similar features in the XANES spectra of the references, they confirmed that Ce(III)-sorbed mixed-layer clay was the reference that can best explain the spectral features of the samples. Extensive sorption of REEs to clays is consistent with the fact that: 1) the mud matrix is composed of clay and silt particles (Yu *et al.* 2015), including minerals like kaolinite, illite, biotite and swelling clays (Astrom and Bjorklund 1997, Yu *et al.* 2015); 2) REEs readily bind to clay minerals (Coppin *et al.* 2002, Huittinen *et al.* 2010, Kynicky *et al.* 2012, Mihajlovic *et al.* 2019); and 3) in

Table 1. Results of a three-step sequential chemical extraction (SCE) applied on La- and Pr-loaded illite, ripidolite and illite-smectite mixed-layer clays. The extractions were done on triplicate samples. The results are presented as mean concentrations ± the standard deviation.

SCE step	Chemical conditions		Illite	Ripidolite	Illite-smectite mixed-layer clay
1	1 M CH_3COONH_4 at pH 6, 4 h	La (ppm)	20 964 ± 158	7799 ± 786	738 ± 68
		Ce (ppm)	4.16 ± 0.54	1.86 ± 0.13	11.0 ± .70
		Pr (ppm)	15412 ± 180	11 205 ± 1256	573 ± 41
2	1 M HCl, 4 h	La (ppm)	1002 ± 32	362 ± 39	24 567 ± 738
		Ce (ppm)	4.93 ± 0.48	0.67 ± 0.07	55.7 ± 1.06
		Pr (ppm)	1068 ± 18.8	885 ± 63.3	16 147 ± 446
3	Concentrated HNO_3, 2h	La (ppm)	97.2 ± 4.43	19.8 ± 0.88	65.9 ± 2.01
		Ce (ppm)	1.19 ± 0.11	BD	45.6 ± 0.90
		Pr (ppm)	83.2 ± 3.67	32.2 ± 0.38	32.8 ± 1.70

regolith profiles elsewhere, REEs are abundantly adsorbed onto clay minerals (Ram *et al.* 2019). Only minor amounts of the REEs were, however, released during the initial three SCE steps targeting, among other phases, weakly adsorbed ions (Fig. 4), which shows that only a minor proportion of the REEs in the mud was weakly bound. This is however not contradicting the XANES results, as previous laboratory experiments demonstrate that under near-neutral to slightly acidic ($pH > 5$) conditions, which prevailed in the estuary, the sorption of REEs by clays such as kaolinite, illite, montmorillonite and smectite occur in the form of inner-sphere surface complexes (Stumpf *et al.* 2002, Coppin *et al.* 2003, Kowal-Fouchard *et al.* 2004, Takahashi *et al.* 2004, Rabung *et al.* 2005). The formation of these surface complexes causes substantial microstructure alterations in the REE-binding environment, that is, a decrease in the number of H_2O molecules in the first coordination shell and the formation of direct binding to a set of adsorption active sites at the edges of clay platelets (Rabung *et al.* 2005, Tan *et al.* 2014). Galunin *et al.* (2011) thus suggests that these REE surface complexes are thermodynamically stable and may be virtually irreversible. In order to test whether clay minerals (phyllosilicates) have the capacity to carry the high REE load of the upper mud unit and that the inner-sphere complexes are not broken until 1 M HCl is applied, three reference clays were doped with La and Pr and extracted sequentially with three reagents. The results showed that for one of the clays (illite-smectite mixed-layer clay) the La and Pr were indeed extensively extracted (96−97%) in Exp_step-2 (1 M HCl), which in assumed to displace inner-sphere complexes, and thus were hardly extractable by Exp_step-1 consisting of 1 M NH_4-acetate at pH 6 (Table 1). For the other two clay minerals (illite and ripidolite), La and Pr extraction was, in contrast, extensive already in Exp_step-1 assumed to displace outer-sphere complexes (92−95%). However, also for illite and ripidolite, the amount of REEs extracted with Exp_step-2 was large (two times higher) relative to the total REE-loading of the upper mud unit and much higher than Ce that was used as a reference for extractability of pristine REEs (associated naturally with the clay). Hence, the results of this relatively simple experiment provided evidence that phyllosilicates indeed have the capacity to be main scavenger phases of the high REE load of the upper mud unit, via formation of inner-sphere complexes.

REE-phosphates were not considered, although these have been identified or indicated in acid sulfate soil landscapes elsewhere (Welch *et al.* 2009, Xu *et al.* 2019). The reason is that in the mud studied here, there is little P and a large excess of Fe(II) relative to sulfide (Yu *et al.* 2015), which means that any available phosphate certainly will have been abundantly trapped by Fe(II) and thus not available for REE binding.

Conclusions

An estuarine sediment (a mud depositional succession) of a creek draining acid sulfate soils had very high REE concentrations (up to 1456 ppm) and accumulation rates (up to 28 g m^{-2} $year^{-1}$) in the upper 182.5 cm, which are estimated to have been deposited between the early 1970s and 2011 (core top). These results, which are in line with previous geochemical studies of soils, waters and suspended-matter in the same setting, are explained by extensive export of acidic waters, rich in dissolved REEs, from acid sulfate soils after these soils became efficiently drained via deep/clean open ditches and subsurface-drainage systems.

Sequential chemical extractions showed that a vast majority of the REEs in the mud samples were released in the acidic 4th step (1 M HCl). This means that the large sedimentary REE pool was only, to a minor extent, bound in clastic phases; but despite that, relatively strongly bound as only minor proportions were extracted with the relatively weak (and pH circumneutral) reagents applied in the first three steps. Cerium XANES spectroscopy and a simple laboratory experiment indicated that the dominating REE-binding phase in the mud was clay minerals, scavenging the REEs via inner-sphere complexation, and additionally ferrihydrite at some depths. This suggested that the REEs transported in dissolved form from the acid sulfate soils are transferred, mainly via relatively strong binding to phyllosilicates, to the particulate phase that ultimately accumulate in the mud. The XANES results should, however, be seen as indicative due to many similar spectral features among the references.

The identified REE concentration features and scavenging mechanisms are of broad practical relevance as acid sulfate soils, which occur mainly on attractive and built low-lying coastal plains, are likely to be even more widespread than presently recognized. Two issues in particular can be highlighted: 1) in the upper two meters of the mud from this study, there was an abundance of acid-extractable (1 M HCl) REEs, which would become highly mobile if the mud was brought into the oxidation zone and thus acidified (via metal-sulfide oxidation) as a result of human activities (e.g. dredging operations) or natural processes; and 2) the total REE concentrations in the mud match very well with the known drainage history and acid sulfate soil development in the catchment, making these metals useful tracers of temporal variations in such activities and processes in coastal settings.

For the Gulf of Bothnia region specifically, where the studied estuary and many other similar acid-sulfate-soil affected estuaries are located, the results show that implementation of modern agricultural drainage techniques in the latter half of the 20th century (deeper/cleaner open ditches and efficient subsurface-drainage systems) considerably increased the leaching of REEs from acid sulfate soils that exist under the farmlands. In the study presented, there are no signs of a decrease in this leaching pattern and consequently there is a need, from an environmental perspective, to develop mitigation strategies so that the leaching of REEs (and other metals) from these environmentally unfriendly soils could be minimized.

Acknowledgements: The XANES measurements were carried out at beamline I811, MAX-Lab, Lund University, Sweden. We thank Dr. Stefan Carlson and Dr. Kajsa Sigfridsson at beamline I811 for their assistance with the XANES measurements. We thank Formas (contract# 2018-00760) and the Geological Survey of Sweden (contract# 36-1878/2017) for financial support.

Supplement: The supplement related to this article is available online at: http://www.borenv.net/BER/archive/pdfs/ber25/ber25-105-120-supplement.pdf

References

Astrom M. 2001. Abundance and fractionation patterns of rare earth elements in streams affected by acid sulphate soils. *Chemical Geology* 175: 249–258.

Astrom M. & Bjorklund A. 1997. Geochemistry and acidity of sulphide-bearing postglacial sediments of western Finland. *Environmental Geochemistry and Health* 19: 155–164.

Astrom M., Sundstrom R., Holmberg M. & Storberg K.E. 2005. pH of streams in western Finland — a perspective from the Middle Ages into the mid 21st century. *Agricultural and Food Science* 14: 5–13.

Astrom M.E., Nystrand M., Gustafsson J.P., Osterholm P., Nordmyr L., Reynolds J.K. & Peltola P. 2010. Lanthanoid behaviour in an acidic landscape. *Geochimica Et Cosmochimica Acta* 74: 829–845.

Astrom M.E., Osterholm P., Gustafsson J.P., Nystrand M., Peltola P., Nordmyr L. & Boman A. 2012. Attenuation of rare earth elements in a boreal estuary. *Geochimica Et Cosmochimica Acta* 96: 105–119.

Astrom M.E., Yu C.X., Peltola P., Reynolds J.K., Osterholm P., Nystrand M.I., Augustsson A., Virtasalo J.J., Nordmyr L. & Ojala A.E.K. 2018. Sources, transport and sinks of beryllium in a coastal landscape affected by acidic soils. *Geochimica Et Cosmochimica Acta* 232: 288–302.

Ayora C., Macias F., Torres E., Lozano A., Carrero S., Nieto J.M., Perez-Lopez R., Fernandez-Martinez A. & Castillo-Michel H. 2016. Recovery of rare earth elements and yttrium from passive-remediation systems of acid mine drainage. *Environmental Science & Technology* 50: 8255–8262.

Bau M. 1999. Scavenging of dissolved yttrium and rare earths by precipitating iron oxyhydroxide: Experimental evidence for Ce oxidation, Y-Ho fractionation, and lanthanide tetrad effect. *Geochimica Et Cosmochimica Acta* 63: 67–77.

Boman A., Frojdo S., Backlund K. & Astrom M.E. 2010. Impact of isostatic land uplift and artificial drainage on oxidation of brackish-water sediments rich in metastable iron sulfide. *Geochimica Et Cosmochimica Acta* 74: 1268–1281.

Borrego J., Carro B., Lopez-Gonzalez N., de la Rosa J., Grande J.A., Gomez T. & de la Torre M.L. 2012. Effect of acid mine drainage on dissolved rare earth elements geochemistry along a fluvial-estuarine system: the Tinto-Odiel Estuary (SW Spain). *Hydrology Research* 43: 262–274.

Brito P., Prego R., Mil-Homens M., Cacador I. & Caetanoa M. 2018. Sources and distribution of yttrium and rare earth elements in surface sediments from Tagus estuary, Portugal. *Science of the Total Environment* 621: 317–325.

Chaillou G., Anschutz P., Lavaux G. & Blanc G. 2006. Rare earth elements in the modern sediments of the Bay of Biscay (France). *Marine Chemistry* 100: 39–52.

Claff S.R., Sullivan L.A., Burton E.D. & Bush R.T. 2010. A sequential extraction procedure for acid sulfate soils:

Partitioning of iron. *Geoderma* 155: 224–230.

Coppin F., Castet S., Berger G. & Loubet M. 2003. Microscopic reversibility of Sm and Yb sorption onto smectite and kaolinite: Experimental evidence. *Geochimica Et Cosmochimica Acta* 67: 2515–2527.

Coppin F., Berger G., Bauer A., Castet S. & Loubet M. 2002. Sorption of lanthanides on smectite and kaolinite. *Chemical Geology* 182: 57–68.

da Silva E.F., Bobos I., Matos J.X., Patinha C., Reis A.P. & Fonseca E.C. 2009. Mineralogy and geochemistry of trace metals and REE in volcanic massive sulfide host rocks, stream sediments, stream waters and acid mine drainage from the Lousal mine area (Iberian Pyrite Belt, Portugal). *Applied Geochemistry* 24: 383–401.

Delgado J., Perez-Lopez R., Galvan L., Nieto J.M. & Boski T. 2012. Enrichment of rare earth elements as environmental tracers of contamination by acid mine drainage in salt marshes: A new perspective. *Marine Pollution Bulletin* 64: 1799–1808.

Dent D.L. & Pons L.J. 1995. A World perspective on acid sulfate soils. *Geoderma* 67: 263–276.

Edahbi M., Plante B., Benzaazoua M., Ward M. & Pelletier M. 2018. Mobility of rare earth elements in mine drainage: Influence of iron oxides, carbonates, and phosphates. *Chemosphere* 199: 647–654.

Freslon N., Bayon G., Toucanne S., Bermell S., Bollinger C., Cheron S., Etoubleau J., Germain Y., Khripounoff A., Ponzevera E. & Rouget M.L. 2014. Rare earth elements and neodymium isotopes in sedimentary organic matter. *Geochimica Et Cosmochimica Acta* 140: 177–198.

Galunin E., Alba M.D., Santos M.J., Abrao T. & Vidal M. 2011. Examination of competitive lanthanide sorption onto smectites and its significance in the management of radioactive waste. *Journal of Hazardous Materials* 186: 1930–1941.

Gammons C.H., Wood S.A. & Nimick D.A. 2005a. Diel behavior of rare earth elements in a mountain stream with acidic to neutral pH. *Geochimica Et Cosmochimica Acta* 69: 3747–3758.

Gammons C.H., Wood S.A., Jonas J.P. & Madison J.P. 2003. Geochemistry of the rare-earth elements and uranium in the acidic Berkeley Pit lake, Butte, Montana. *Chemical Geology* 198: 269–288.

Gammons C.H., Wood S.A., Pedrozo F., Varekamp J.C., Nelson B.J., Shope C.L. & Baffico G. 2005b. Hydrogeochemistry and rare earth element behavior in a volcanically acidified watershed in Patagonia, Argentina. *Chemical Geology* 222: 249–267.

Gladysz-Plaska A., Majdan M. & Grabias E. 2014. Adsorption of La, Eu and Lu on raw and modified red clay. *Journal of Radioanalytical and Nuclear Chemistry* 301: 33–40.

Grafe M., Donner E., Collins R.N. & Lombi E. 2014. Speciation of metal(loid)s in environmental samples by X-ray absorption spectroscopy: A critical review. *Analytica Chimica Acta* 822: 1–22.

Groger J., Proske U., Hanebuth T.J.J. & Hamer K. 2011. Cycling of trace metals and rare earth elements (REE) in acid sulfate soils in the Plain of Reeds, Vietnam. *Chemical Geology* 288: 162–177.

Gromet L.P., Dymek R.F., Haskin L.A. & Korotev R.L. 1984. The North-American shale composite: its compilation, major and trace-element characteristics. *Geochimica Et Cosmochimica Acta* 48: 2469–2482.

Haese R.R., Wallmann K., Dahmke A., Kretzmann U., Müller P.J. & H.D. S. 1997. Iron species determination to investigate early diagenetic reactivity in marine sediments. *Geochimica et Cosmochimica Acta* 61: 63–72.

Haskin L.A., Haskin M.A., Frey F.A., Wilderman T.R. 1968. Relative and absolute terrestrial abundance of the rare earths. In: L.H. A. (ed.), Origin and distribution of the elements, Pergamon, Oxford, pp. 889–912.

Huittinen N., Rabung T., Andrieux P., Lehto J. & Geckeis H. 2010. A comparative batch sorption and time-resolved laser fluorescence spectroscopy study on the sorption of Eu(III) and Cm(III) on synthetic and natural kaolinite. *Radiochimica Acta* 98: 613–620.

Johnston S.G., Rose A.L., Burton E.D. & Webster-Brown J. 2015. Landslide-induced iron mobilisation shapes benthic accumulation of nutrients, trace metals and REE fractionation in an oligotrophic alpine stream. *Geochimica Et Cosmochimica Acta* 148: 1–22.

Jones A.M., Xue Y.J., Kinsela A.S., Wilcken K.M. & Collins R.N. 2016. Donnan membrane speciation of Al, Fe, trace metals and REEs in coastal lowland acid sulfate soil-impacted drainage waters. *Science of the Total Environment* 547: 104–113.

Kowal-Fouchard A., Drot R., Simoni E., Marmier N., Fromage F. & Ehrhardt J.J. 2004. Structural identification of europium(III) adsorption complexes on montmorillonite. *New Journal of Chemistry* 28: 864–869.

Kynicky J., Smith M.P. & Xu C. 2012. Diversity of Rare Earth Deposits: The Key Example of China. *Elements* 8: 361–367.

Lawrence M.G., Greig A., Collerson K.D. & Kamber B.S. 2006. Rare earth element and yttrium variability in South East Queensland waterways. *Aquatic Geochemistry* 12: 39–72.

Lecomte K.L., Sarmiento A.M., Borrego J. & Nieto J.M. 2017. Rare earth elements mobility processes in an AMD-affected estuary: Huelva Estuary (SW Spain). *Marine Pollution Bulletin* 121: 282–291.

Li X.X. & Wu P. 2017. Geochemical characteristics of dissolved rare earth elements in acid mine drainage from abandoned high-As coal mining area, southwestern China. *Environmental Science and Pollution Research* 24: 20540–20555.

Lombi E. & Susini J. 2009. Synchrotron-based techniques for plant and soil science: opportunities, challenges and future perspectives. *Plant and Soil* 320: 1–35.

Lozano A., Ayora C. & Fernandez-Martinez A. 2020. Sorption of rare earth elements on schwertmannite and their mobility in acid mine drainage treatments. *Applied Geochemistry* 113.

Lozano A., Fernandez-Martinez A., Ayora C., Di Tommaso D., Poulain A., Rovezzi M. & Marini C. 2019. Solid and Aqueous Speciation of Yttrium in Passive Remediation Systems of Acid Mine Drainage. *Environmental Science & Technology* 53: 11153–11161.

Manceau A. & Matynia A. 2010. The nature of Cu bonding to natural organic matter. *Geochimica Et Cosmochimica Acta* 74: 2556–2580.

Marsac R., Davranche M., Gruau G., Bouhnik-Le Coz M. & Dia A. 2011. An improved description of the interactions between rare earth elements and humic acids by modeling: PHREEQC-Model VI coupling. *Geochimica Et Cosmochimica Acta* 75: 5625–5637.

Mihajlovic J., Bauriegel A., Stark H.J., Rosskopf N., Zeitz J., Milbert G. & Rinklebe J. 2019. Rare earth elements in soil profiles of various ecosystems across Germany. *Applied Geochemistry* 102: 197–217.

Moraes M.L.B., Murciego A., Alvarez-ayuso E. & Ladeira A.C.Q. 2020. The role of Al-13-polymers in the recovery of rare earth elements from acid mine drainage through pH neutralization. *Applied Geochemistry* 113.

Morgan B., Rate A.W., Burton E.D. & Smirk M.N. 2012. Enrichment and fractionation of rare earth elements in FeS-rich and organic-rich estuarine sediments receiving acid sulfate soil drainage. *Chemical Geology* 308-309: 60–73.

Morgan B., Johnston S.G., Burton E.D. & Hagan R.E. 2016. Acidic drainage drives anomalous rare earth element signatures in intertidal mangrove sediments. *Science of the Total Environment* 573: 831–840.

Mosley L.M., Palmer D., Leyden E., Cook F., Zammit B., Shand P., Baker A. & Fitzpatrick R.W. 2014. Acidification of floodplains due to river level decline during drought. *Journal of Contaminant Hydrology* 161: 10–23.

Neaman A., Mouélé F., Trolard F. & Bourrié G. 2004. Improved methods for selective dissolution of Mn oxides: applications for studying trace element associations. *Applied Geochemistry* 19: 973–979.

Noack C.W., Dzombak D.A. & Karamalidis A.K. 2014. Rare Earth Element Distributions and Trends in Natural Waters with a Focus on Groundwater. *Environmental Science & Technology* 48: 4317–4326.

Nordmyr L., Astrom M. & Peltola P. 2008a. Metal pollution of estuarine sediments caused by leaching of acid sulphate soils. *Estuarine Coastal and Shelf Science* 76: 141–152.

Nordmyr L., Osterholm P. & Astrom M. 2008b. Estuarine behaviour of metal loads leached from coastal lowland acid sulphate soils. *Marine Environmental Research* 66: 378–393.

Ogawa Y., Ishiyama D., Shikazono N., Iwane K., Hoshino T., Kajiwara M., Tsuchiya N., Saini-Eidukat B. & Wood S.A. 2019. Fractionation of rare earth elements (REEs) and actinides (U and Th) originating from acid thermal water during artificial and natural neutralization processes of surface waters. *Geochimica Et Cosmochimica Acta* 249: 247–262.

Olias M., Canovas C.R., Basallote M.D. & Lozano A. 2018. Geochemical behaviour of rare earth elements (REE) along a river reach receiving inputs of acid mine drainage. *Chemical Geology* 493: 468–477.

Osterholm P. & Astrom M. 2002. Spatial trends and losses of major and trace elements in agricultural acid sulphate soils distributed in the artificially drained Rintala area, W. Finland. *Applied Geochemistry* 17: 1209–1218.

Pourret O. & Martinez R.E. 2009. Modeling lanthanide series binding sites on humic acid. *Journal of Colloid and Interface Science* 330: 45–50.

Pourret O., Davranche M., Gruau G. & Dia A. 2007. Rare earth elements complexation with humic acid. *Chemical Geology* 243: 128–141.

Protano G. & Riccobono F. 2002. High contents of rare earth elements (REES) in stream waters of a Cu-Pb-Zn mining area. *Environmental Pollution* 117: 499–514.

Quinn K.A., Byrne R.H. & Schijf J. 2004. Comparative scavenging of yttrium and the rare earth elements in seawater: Competitive influences of solution and surface chemistry. *Aquatic Geochemistry* 10: 59–80.

Quinn K.A., Byrne R.H. & Schijf J. 2006. Sorption of yttrium and rare earth elements by amorphous ferric hydroxide: Influence of pH and ionic strength. *Marine Chemistry* 99: 128–150.

Rabung T., Pierret M.C., Bauer A., Geckeis H., Bradbury M.H. & Baeyens B. 2005. Sorption of Eu(III)/Cm(III) on Ca-montmorillonite and Na-illite. Part 1: Batch sorption and time-resolved laser fluorescence spectroscopy experiments. *Geochimica Et Cosmochimica Acta* 69: 5393–5402.

Ram R., Becker M., Brugger J., Etschmann B., Burcher-Jones C., Howard D., Kooyman P.J. & Petersen J. 2019. Characterisation of a rare earth element- and zirconium-bearing ion-adsorption clay deposit in Madagascar. *Chemical Geology* 522: 93–107.

Ramsey, B.C. 2009. Bayesian analysis of radiocarbon dates. *Radiocarbon*, 51(1), 337–360.

Roos M. & Astrom M. 2005. Hydrochemistry of rivers in an acid sulphate soil hotspot area in western Finland. *Agricultural and Food Science* 14: 24–33.

Scheinost A.C., Kretzschmar R. & Pfister S. 2002. Combining Selective Sequential Extractions, X-ray Absorption Spectroscopy, and Principal Component Analysis for Quantitative Zinc Speciation in Soil. *Environmental Science & Technology* 36: 5021–5028.

Sholkovitz E.R. 1995. The aquatic chemistry of rare earth elements in rivers and estuaries. *Aquatic Geochemistry* 1: 1–34.

Sholkovitz E.R., Shaw T.J. & Schneider D.L. 1992. The geochemistry of rare-earth elements in the seasonally anoxic water column and porewaters of Chesapeake Bay. *Geochimica Et Cosmochimica Acta* 56: 3389–3402.

Sohlenius G. & Oborn I. 2004. Geochemistry and partitioning of trace metals in acid sulphate soils in Sweden and Finland before and after sulphide oxidation. *Geoderma* 122: 167–175.

Soyol-Erdene T.O., Valente T., Grande J.A. & de la Torre M.L. 2018. Mineralogical controls on mobility of rare earth elements in acid mine drainage environments. *Chemosphere* 205: 317–327.

Stewart B.W., Capo R.C., Hedin B.C. & Hedin R.S. 2017. Rare earth element resources in coal mine drainage and treatment precipitates in the Appalachian Basin, USA. *International Journal of Coal Geology* 169: 28–39.

Stroeven A.P., Hattestrand C., Kleman J., Heyman J., Fabel D., Fredin O., Goodfellow B.W., Harbor J.M., Jansen J.D., Olsen L., Caffee M.W., Fink D., Lundqvist J., Rosqvist G.C., Stromberg B. & Jansson K.N. 2016. Deglaciation of Fennoscandia. *Quaternary Science Reviews* 147: 91−121.

Stumpf T., Bauer A., Coppin F., Fanghanel T. & Kim J.I. 2002. Inner-sphere, outer-sphere and ternary surface complexes: a TRLFS study of the sorption process of Eu(III) onto smectite and kaolinite. *Radiochimica Acta* 90: 345−349.

Sukitprapanon T.S., Suddhiprakarn A., Kheoruenromne I. & Gilkes R.J. 2019. Rare earth elements in acid sulfate soils under long-term paddy rice cultivation in Thailand. *Geoderma Regional* 17.

Sundstrom R., Astrom M. & Osterholm P. 2002. Comparison of the metal content in acid sulfate soil runoff and industrial effluents in Finland. *Environmental Science & Technology* 36: 4269−4272.

Takahashi Y., Tada A. & Shimizu H. 2004. Distribution pattern of rare earth ions between water and montmorillonite and its relation to the sorbed species of the ions. *Analytical Sciences* 20: 1301−1306.

Tan X., Ren X., Chen C. & Wang X. 2014. Analytical approaches to the speciation of lanthanides at solid-water interfaces. *TrAC Trends in Analytical Chemistry* 61: 107−132.

Tang J.W. & Johannesson K.H. 2010. Ligand extraction of rare earth elements from aquifer sediments: Implications for rare earth element complexation with organic matter in natural waters. *Geochimica Et Cosmochimica Acta* 74: 6690−6705.

Tertre E., Hofmann A. & Berger G. 2008. Rare earth element sorption by basaltic rock: Experimental data and modeling results using the "Generalised Composite approach". *Geochimica Et Cosmochimica Acta* 72: 1043−1056.

Verplanck P.L., Nordstrom D.K., Taylor H.E. & Kimball B.A. 2004. Rare earth element partitioning between hydrous ferric oxides and acid mine water during iron oxidation. *Applied Geochemistry* 19: 1339−1354.

Wallin J., Karjalainen A.K., Schultz E., Järvistö J., Leppänen M. & Vuori K.M. 2015. Weight-of-evidence approach in assessment of ecotoxicological risks of acid sulphate soils in the Baltic Sea river estuaries. *Science of the Total Environment* 508: 452−461.

Wallrich I.L.R., Stewart B.W., Capo R.C., Hedin B.C. & Phan T.T. 2020. Neodymium isotopes track sources of rare earth elements in acidic mine waters. *Geochimica Et Cosmochimica Acta* 269: 465−483.

Welch S.A., Christy A.G., Isaacson L. & Kirste D. 2009. Mineralogical control of rare earth elements in acid sulfate soils. *Geochimica Et Cosmochimica Acta* 73: 44−64.

Wood S.A., Garnmons C.H. & Parker S.R. 2006. The behavior of rare earth elements in naturally and anthropogenically acidified waters. *Journal of Alloys and Compounds* 418: 161−165.

Xu N., Morgan B. & Rate A.W. 2018. From source to sink: rare-earth elements trace the legacy of sulfuric dredge spoils on estuarine sediments. *Science of the Total Environment* 637: 1537−1549.

Xu N., Rate A.W., Morgan B. & Saunders M. 2019. Micro- and Nanoscale identification of Rare Earth Element-Mineral Associations in an Acidified Dredge Spoil and Adjacent Reduced Sediments. *ACS Earth and Space Chemistry* 3: 51−61.

Yli-Halla M., Puustinen M. & Koskiaho J. 1999. Area of cultivated acid sulfate soils in Finland. *Soil Use and Management* 15: 62−67.

Yu C.X., Virtasalo J.J., Österholm P., Burton E.D., Peltola P., Ojala A.E.K., Hogmalm J.K. & Astrom M.E. 2016a. Manganese accumulation and solid-phase speciation in a 3.5 m thick mud sequence from the estuary of an acidic and Mn-rich creek, northern Baltic Sea. *Chemical Geology* 437: 56−66.

Yu C.X., Peltola P., Nystrand M.I., Virtasalo J.J., Österholm P., Ojala A.E.K., Hogmalm J.K. & Astrom M.E. 2016b. Arsenic removal from contaminated brackish sea water by sorption onto Al hydroxides and Fe phases mobilized by land-use. *Science of the Total Environment* 542: 923−934.

Yu C.X., Virtasalo J.J., Karlsson T., Peltola P., Österholm P., Burton E.D., Arppe L., Hogmalm J.K., Ojala A.E.K. & Astrom M.E. 2015. Iron behavior in a northern estuary: Large pools of non-sulfidized Fe(II) associated with organic matter. *Chemical Geology* 413: 73−85.

Zhong S.J. & Mucci A. 1995. Partitioning of rare-earth elements (REEs) between calcite and seawater solutions at 25° C and 1 atm, and high dissolved REE concentrations. *Geochimica Et Cosmochimica Acta* 59: 443−453.